Optimal transmission schemes in wireless networks and their comparison with simple ALOHA based scheme

Philippe Jacquet, Salman Malik

▶ **To cite this version:**

Philippe Jacquet, Salman Malik. Optimal transmission schemes in wireless networks and their comparison with simple ALOHA based scheme. [Research Report] RR-7339, INRIA. 2010. inria-00504081v2

HAL Id: inria-00504081

https://hal.inria.fr/inria-00504081v2

Submitted on 28 Jul 2010

INRIA

Optimal transmission schemes in wireless networks and their comparison with simple ALOHA based scheme

Philippe Jacquet — Salman Malik

N° 7339

July 2010

___ Networks and Telecommunications ___

Rapport de recherche

Optimal transmission schemes in wireless networks and their comparison with simple ALOHA based scheme

Philippe Jacquet , Salman Malik

Abstract: We present our analysis and results that allow us to conjecture that maximum capacity in wireless networks can be achieved if nodes transmitting simultaneously are positioned in a hexagonal grid pattern. But obviously, it is very difficult to realize such a protocol which ensures that active transmitters in the network are positioned in any specific grid pattern. We compare the optimal capacity in networks with grid positioned transmitters with the capacity of wireless networks where nodes are dispatched according to uniform distribution and use very simple ALOHA-based protocol for channel access. We will also extend this analysis to multi-hop case and characterize the maximum throughput achievable in wireless networks with ALOHA-based protocols and TDMA and grid based TDMA protocols.

Key-words: single-hop network, multi-hop network, capacity, throughput, slotted ALOHA, TDMA, Grid based TDMA, square, hexagonal, honeycomb

Protocoles optimaux de transmission dans les réseaux sans fil et comparaisons avec des protocoles basés sur ALOHA

Résumé : Nous présentons une analyse et des résultats qui nous permettent de conjecturer que la capacité maximale dans les réseaux sans fil est obtenue quand les noeuds transmettant simultanément sont placés dans une configuration de grille hexagonale. Naturellement, il est très difficile de réaliser en pratique un protocole qui s'assure que des émetteurs actifs dans le réseau soient placés dans une topologie spécifique en grille. L'objet de ce rapport est de comparer la capacité optimale dans les réseaux avec des émetteurs placés en grille avec la capacité de réseaux sans fil où des noeuds sont placés selon la distribution uniforme et utilisent un protocole ALOHA très simple pour l'accès au medium. Nous étendons l'analyse au cas multi-sauts et nous caractérisons le capacité maximale utilisable dans les réseaux sans fil avec des protocoles ALOHA, des protocoles TDMA et des protocoles de TDMA organisś en grille.

Mots-clés : multi-saut réseau, capacité, protocoles TDMA, protocoles de TDMA organisés en grille

1 Introduction

Performance in multi-hop networks is in general poor compared to nominal bandwidth. This is mainly due to the interference management which can effect the spatial reuse of wireless channel over the multi-hop path. In future, wireless networks are expected to be deployed widely and the question is how these networks can satisfy the increasing demand on throughput under these constraints. Many of the proposed protocols for optimizing throughput in wireless networks use channel reservation or node coloring schemes, for example [4,5,12,13]. Such protocols can be very complex to implement in real world.

In this report we will be characterizing the throughput of wireless networks under different protocols which can be a challenging task especially under multi-hop conditions. We will investigate how TDMA based protocols compare with much simpler ALOHA-based protocols. We will also evaluate the grid based TDMA protocol which ensures that simultaneous transmitters are positioned in a specific grid pattern to give maximum throughput in a wireless network. Wireless networks of regular grid topologies are studied in, for example, [7,10] and compared to networks with randomly dispatched nodes. In our analysis of grid based TDMA, only the transmitters accessing the channel simultaneously form a regular grid pattern. Our aim is to lay the groundwork for the design of simpler protocols for multi-hop adhoc networks and the main result from this report is that complex reservation protocols like TDMA or grid based TDMA do not significantly improve the throughput in wireless networks as compared to the simple slotted ALOHA protocol.

This report is organized as follows. In the next section, we present the comparison of Poisson distributed networks and grid-based networks in terms of average information rate that any arbitrarily placed node can receive. We limit our analysis to the case where a node can receive at most one packet at a time provided its signal-to-noise ratio (SNR) condition is fulfilled. We extend our analysis to multi-hop case and evaluate maximum throughput of different protocols in section 3. In the last section 4, we analyze the optimality of grid arranged field of transmitters.

2 Capacity with randomly and grid positioned transmitters

The authors of [6] have shown that information rate received by every node is finite and is irrespective of the network density. This analysis was done under the hypothesis that a node can only receive from one transmitter at a time. An accurate assessment of the capacity of a wireless network shall take into account:

1. Geometry for positioning of the nodes

2. Physics for wave propagation and attenuation in the medium and

3. Information theory for extraction of information from received signal.

Article [8] evaluates the capacity of a wireless network in a realistic model. From explicit formula of the Laplace transform of received signal distribution, it derives an explicit formula for the average information rate received by a

random node under the assumption that transmitters are dispatched over an infinite plane according to the Poisson distribution. This model involves the above mentioned three aspects in the following manner:

1. Nodes are distributed over the network plane according to uniform distribution and use any nominal transmit power

2. Attenuation is related to distance: $\frac{1}{r^\alpha}$ and random fading and

3. Information is extracted from parallel superimposed signals in a similar way as in multiple-input-multiple-output technology (MIMO).

It can be argued that the optimal positioning of transmitters in a network shall be the grid formation. This optimal positioning can be achieved under a hypothetical medium access protocol but designing such a protocol is very difficult because of the limitations introduced by wave propagation characteristics and node distribution and is beyond the scope of this report. In this section we analyze the networks with transmitters optimally positioned in square, hexagonal and honeycomb grids. We compare these results with [8] and limit to the case when at most one packet, satisfying the SNR condition, is received successfully. We are not considering the MIMO situation where a node can receive several packets simultaneously.

Our comparison is in terms of the average information rate received by an arbitrarily placed Access Point (AP) in the network. An important result from this analysis is that information rate received by the AP is maximum when transmitters are positioned in hexagonal grid and is comparable albeit slightly higher than the average information rate received if the transmitters are distributed randomly.

In section 2.1 we present the main results from [8]. Evaluation of grid-based networks is discussed in section 2.2 and results from our numerical simulations are presented in the section 2.3.

We assume that fading is zero and we restrict to uniform unit nominal transmit power.

2.1 Model for protocols based on randomly distributed transmitters

Consider an infinite network on $2D$ plane with nodes randomly distributed.

We consider the following model for this network:

1. time is slotted

2. nodes are synchronized and use slotted ALOHA protocol

3. in each slot, nodes which simultaneously transmit are given by a uniform Poisson distribution of mean λ transmitters per unit square area.

This model has been investigated in detail in [8]. In order to make this report self contained, we will summarize some of the analytical results from [8].

We assume that the attenuation coefficient (α) is greater than 2.

The signal level of a transmission received at distance r is: $\frac{1}{r^\alpha}$.

If $\mathcal{S}$ is the set of the locations of all transmitters, and $z_i \in \mathcal{S}$ is the transmitter whose SNR at location z should be at least equal to K then:

$$|z - z_i|^{-\alpha} \geq K \sum_{j \neq i} |z - z_j|^{-\alpha} \tag{1}$$

where $|z|$ represents the Euclidean norm of a vector $z = (x, y) : |z| = \sqrt{x^2 + y^2}$.

or $W(z, \{z_i\}) \geq KW(z, \mathcal{S} - \{z_i\})$ where $W(z, S) = \sum_{z_j \in S} |z - z_j|^{-\alpha}$.
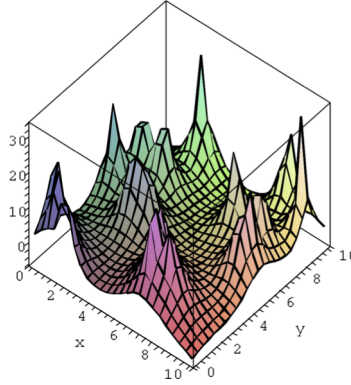
2.1.1 Distribution of signal levels

Figure 1: Signal Levels (in dB's) for a random network with attenuation coefficient $\alpha = 2.5$

Figure 1 shows the function $W(z, \mathcal{S})$ for z varying in the plane with $\mathcal{S}$ an arbitrary set of Poisson distributed transmitters. Figure 1 uses $\alpha = 2.5$. It is clear that closer the receiver is to the transmitter, larger is the SNR. For each value of K we can draw an area, around each transmitter, where its signal can be received with SNR greater or equal to K. Figure 2 shows reception areas for the same set $\mathcal{S}$, as in Figure 1, for various values of K. As can be seen, the reception areas do not overlap for $K > 1$ since there is only one dominant signal. For each value of K we can draw, around each transmitter, the area where its signal is received with SNR greater or equal to K. The aim is to find the average size of this area and how it is a function of λ, K and α.

$W(z, \mathcal{S})$ depends on $\mathcal{S}$ and hence is also a random variable. The random variable $W(z, \mathcal{S})$ has a distribution which is invariant by translation and therefore does not depend on z. Let $w(\mathcal{S})$ be its density function. If $\mathcal{S}$ is given by a $2D$ Poisson process with intensity λ transmitters per slot per unit square area, Laplace transform of $w(\mathcal{S})$, $\tilde{w}(\theta, \lambda)$, can be computed exactly.

The Laplace transform, $\tilde{w}(\theta, \lambda) = \exp(\int (e^{-\theta r^{-\alpha}} - 1) r dr$, satisfies the identity:

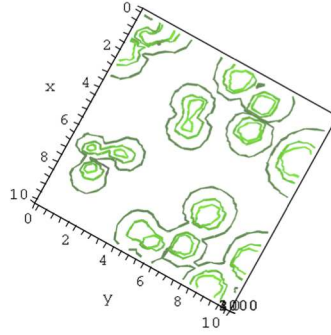$$\tilde{w}(\theta, \lambda) = \exp(\pi \lambda \Gamma(1 - \frac{2}{\alpha}) \theta^{\frac{2}{\alpha}})$$

Figure 2: Distribution of reception areas for various value of SNR. $K = 1, 4, 10$ for situation of figure 1

From the above formula and by applying inverse Laplace transformation:

$$P(W(\lambda) < x) = \frac{1}{2i\pi} \int\limits_{-i\infty}^{+i\infty} \frac{\tilde{w}(\theta, \lambda)}{\theta} e^{\theta x} d\theta$$

Expanding $\tilde{w}(\theta, \lambda) = \sum\limits_{n \geq 0} \frac{(-C\lambda)^n}{n!} \theta^{n\gamma}$

$$P(W(\lambda) < x) = \frac{1}{2i\pi} \sum\limits_{n \geq 0} \frac{(-C\lambda)^n}{n!} \int\limits_{-i\infty}^{+i\infty} \theta^{n\gamma-1} e^{\theta x} d\theta$$

Then by bending the integration path towards negative axis:

$$\frac{1}{2i\pi} \int\limits_{-i\infty}^{+i\infty} \theta^{n\gamma-1} e^{\theta x} d\theta = \frac{e^{i\pi n\gamma} - e^{-i\pi n\gamma}}{2i\pi} \int\limits_{0}^{\infty} \theta^{n\gamma-1} e^{-\theta x} d\theta$$

$$= \frac{\sin(\pi n\gamma)}{\pi} \Gamma(n\gamma) x^{-n\gamma}$$

we get,

$$P(W(\lambda) < x) = \sum\limits_{n \geq 0} \frac{(-C\lambda)^n}{n!} \frac{\sin(\pi n\gamma)}{\pi} \Gamma(n\gamma) x^{-n\gamma} \tag{2}$$

where $\gamma = \frac{2}{\alpha}$ and $\Gamma(.)$ is the Gamma function.

2.1.2 Reception areas

Let $p(\lambda, r, K, \alpha)$ be the probability to receive a signal sent at distance r with SNR at least equal to K. Then: $p(\lambda, r, K, \alpha) = P(W(\lambda) < \frac{r^{-\alpha}}{K})$ and average

size of the reception area around an arbitrary transmitter with SNR at least equal to K is: $\sigma(\lambda, K, \alpha) = 2\pi \int p(\lambda, r, K, \alpha) r dr$.

The average size of the reception area around an arbitrary transmitter i with SNR at least equal to K satisfies the identity:

$$\sigma_i(\lambda, K, \alpha) = \frac{1}{\lambda} \frac{\sin(\frac{2}{\alpha}\pi)}{\frac{2}{\alpha}\pi} K^{-\frac{2}{\alpha}} \qquad (3)$$

The reception area $\sigma_i(\lambda, K, \alpha)$ is inversely proportional to the density of transmitters λ and the product $\lambda\sigma_i(\lambda, K, \alpha)$ is a function of K and α.

We notice that when $\alpha \to \infty$, $\sigma_i(\lambda, K, \infty) \to \frac{1}{\lambda}$. This is due to the fact that when α is very large, closest node acting as source of interference gives the far largest estimate and consequently the area of reception turns to be Voronoi cell around each transmitter. This holds for all values of K. The average size of Voronoi cell being equal to the inverse density of the transmitters, $\frac{1}{\lambda}$, we get the asymptotic result. Note that when K grows as $\exp(O(\alpha))$, we have $\sigma_i(\lambda, K, \alpha) \approx \frac{1}{\lambda} \exp(-\frac{2}{\alpha} \log(K))$, which suggests that the typical SNR as $\alpha \to \infty$ is of the order of $\exp(O(\alpha))$.

Secondly, as $\alpha \to 2$, we have $\sigma_i(\lambda, K, 2) \to 0$ because $\sin(\frac{2}{\alpha}\pi) \to 0$. Indeed, the contribution of remote nodes tends to diverge and makes the SNR approach to zero. This explains why $\sigma_i(\lambda, K, 2) \to 0$ for any fixed value of K.

2.1.3 Capacity of wireless networks with Poisson distributed transmitters

Consider an AP at an arbitrary location z and let $N(z, \lambda, K, \alpha)$ denote the number of K-reception areas it belongs to. The quantity $N(z, \lambda, K, \alpha)$ is sometimes called the K-hand-over number of the AP. Following theorem has been proved in [1,8]:

$$E(N(z, \lambda, K, \alpha)) = \lambda\sigma_i(\lambda, K, \alpha) = \sigma_i(1, K, \alpha) \qquad (4)$$

$E(N(z, \lambda, K, \alpha))$ represents the average number of associations of an arbitrarily placed AP in the network. Under the hypothesis that a node can only receive at most one packet at a time, the average information rate received by the AP is also equal to $E(N(z, \lambda, K, \alpha))$.

Note that $E(N(z, \lambda, K, \alpha))$ is independent of λ and

$$\lim_{\alpha \to \infty} E(N(z, \lambda, K, \alpha)) \to 1.$$

2.2 Model for protocols based on transmitters positioned in grid formation

Consider an infinite $2D$ plane with transmitters distributed like a sequence of points $(z_1, z_2, z_3, ...)$ and arranged in grid formation where $z_i = (x_i, y_i)$ is the location of transmitter number i.

We consider the following model for this network:

1. time is slotted and

2. in each slot, all transmitters will transmit simultaneously.
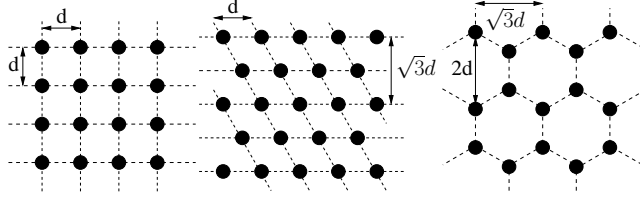
Figure 3: Square, Hexagonal and Honey-Comb grid layouts

In our analysis, we have covered grid layouts of square, hexagonal and honeycomb as shown in figure 3. Grids are constructed from d which defines the minimum distance in-between neighboring transmitters and can be derived from hop-distance parameter of a typical TDMA-based protocol. The actual meaning of the value of d is beyond the scope of this section. The density of transmitters, λ, is the number of grid points (transmitters) per unit square area. λ will depend on the type of grid layout and will be inversely proportional to d^2.

We are not aware of any analytical formula, as derived for the case of network with Poisson distributed transmitters, for the size of reception areas in grid networks. Therefore we have used a numerical method for computing the size of reception area around an arbitrary transmitter in the network.

2.2.1 Reception areas

Our aim is to find the area, the size of set of points $A_i(\lambda, K, \alpha)$, where signal from transmitter i is received with SNR at least equal to K. Here noise is the sum of received signal power from all transmitters excluding i.

Now there can be two approaches for computing the size of reception area. First approach uses the Monte Carlo simulation method while the second approach involves computing the size of reception area via numerical integration. While we have implemented both approaches, the problem with Monte Carlo simulation method is that we are not able to get sufficiently accurate results because of the sampling error. Therefore, herein we will only present the numerical integration approach.

The set $A_i(\lambda, K, \alpha)$ contains the point z_i since here the SNR is infinite.
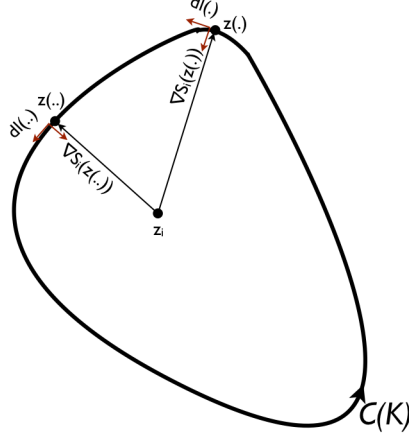
Our aim is to compute $\sigma_i(\lambda, K, \alpha) = |A_i(\lambda, K, \alpha)|$.

If $\mathcal{C}(K, \alpha)$ is the closed curve that makes the boundary of $\sigma_i(\lambda, K, \alpha)$ and z is a point on $\mathcal{C}(K, \alpha)$, we have

$$\sigma_i(\lambda, K, \alpha) = \frac{1}{2} \int_{\mathcal{C}(K,\alpha)} \det(z - z_i, dl) \tag{5}$$

where $\det(a, b)$ is the determinant of vectors a and b. Here it gives the area of the parallelogram formed by the two vectors.

In equation 5, dl is the vector tangent to $\mathcal{C}(K, \alpha)$ at point z. $\mathcal{C}(K, \alpha)$ is assumed counter-clockwise such that area $\sigma_i(\lambda, K, \alpha)$ is always on its left. Note

Figure 4: Computation of size of reception area of transmitter i

that equation 5 remains true if z_i is replaced by any interior point of $\sigma_i(\lambda, K, \alpha)$. From equation 1, SNR $S_i(z)$ of transmitter i at point z can be written as:

$$S_i(z) = \frac{|z - z_i|^{-\alpha}}{\sum\limits_{j \neq i} |z - z_j|^{-\alpha}} \tag{6}$$

We can assume that at point z, $S_i(z) = K$.

On point z we can define the gradient of $S_i(z)$, $\nabla S_i(z) = \begin{bmatrix} \frac{\partial}{\partial x} S_i(z) \\ \frac{\partial}{\partial y} S_i(z) \end{bmatrix}$. Details on computing $\nabla S_i(z)$ can be found in appendix.

The vector dl, tangent to $\mathcal{C}(K, \alpha)$ at point z, is co-linear with $J \frac{\nabla S_i(z)}{||\nabla S_i(z)||}$ where J is the rotation matrix, $J = \begin{bmatrix} 0 & 1 \\ -1 & 0 \end{bmatrix}$ and $||.||$ is the magnitude of the vector (to align with the direction of $\mathcal{C}(K, \alpha)$, $\nabla S_i(z)$ is rotated clockwise).

Therefore, we can fix $dl = J \frac{\nabla S_i(z)}{||\nabla S_i(z)||} \delta t$ and in equation 5,

$$\det(z - z_i, dl) = -(z - z_i) . \frac{\nabla S_i(z)}{||\nabla S_i(z)||} \delta t$$

$$= -(x - x_i) \frac{\frac{\partial}{\partial x} S_i(z)}{||\nabla S_i(z)||} \delta t - (y - y_i) \frac{\frac{\partial}{\partial y} S_i(z)}{||\nabla S_i(z)||} \delta t$$

where $\delta t \to 0$.

The sequence of points $z(k)$, computed as

$$z(0) = z$$

$$z(1) = z(0) + J\frac{\nabla S_i(z(0))}{||\nabla S_i(z(0))||}\delta t$$

$$z(k+1) = z(k) + J\frac{\nabla S_i(z(k))}{||\nabla S_i(z(k))||}\delta t$$

describes $\mathcal{C}(K, \alpha)$ when $\delta t \to 0$.

Therefore the expression 5 reduces to,

$$\sigma_i(\lambda, K, \alpha) = \frac{1}{2}\int\limits_{\mathcal{C}(K,\alpha)} \det(z - z_i, dl) \tag{7}$$

$$\approx -\frac{1}{2}\sum_k (z(k) - z_i).\frac{\nabla S_i(z(k))}{||\nabla S_i(z(k))||}\delta t$$

assuming that we stop the sequence $z(k)$ when it loops back on or close to the point z. Details on how to find the first point $z(0) = z$ can be found in Appendix. Note that the negative sign in equation 7 is automatically negated by the dot product of vectors $z(k) - z_i$ and $\nabla S_i(z(k))$.

2.2.2 Capacity of wireless networks with transmitters positioned in grid patterns

As we do not have a closed form expression for the reception area $\sigma_i(\lambda, K, \alpha)$,

$$N(z, \lambda, K, \alpha) = \lambda\sigma_i(\lambda, K, \alpha)$$

is computed numerically according to the method described above.

2.3 Numerical simulations

In this section we will compare grid networks where transmitters are arranged in square, hexagonal and honeycomb patterns respectively with network where transmitters are Poisson distributed.

The comparison is in terms of $E(N(z, \lambda, K, \alpha)) = \lambda\sigma_i(\lambda, K, \alpha)$.

For grid arranged transmitters, we performed numerical simulations in a very large network spread over $2D$ square area with length of each side equal to 5000 meters. Transmitters are spread over this area in square, hexagonal or honeycomb pattern. To avoid edge affects, the transmitter i, whose reception area we will compute, is located in the center at origin, $z_i = (x_i, y_i) = (0, 0)$. The network area is large enough so that the transmitters on the boundary have almost negligible effect on the reception area of transmitter i. We set d equal to 30 meters although it will have no effect on the validity of our conclusions as $\lambda\sigma_i(\lambda, K, \alpha)$ is independent of λ. In our numerical simulations, we set $\delta t = 0.01$. λ depends on the type of grid and is computed from the total number of transmitters spread over the network area of 5000 x 5000 square meters.

In case of randomly distributed transmitters, $\lambda\sigma_i(\lambda, K, \alpha) = \sigma_i(1, K, \alpha)$ is computed from the analytic expression 3.
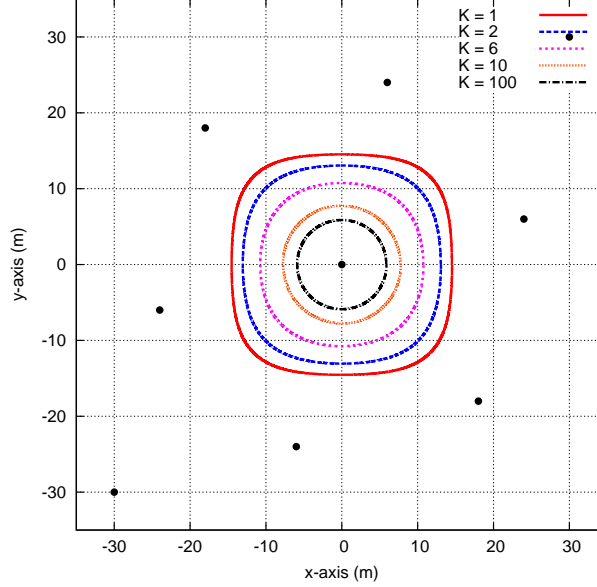
Figure 5: Reception Area in Square Grid network with varying K - $d = 30m$, $\alpha = 4.0$

2.3.1 Comparison with varying SNR

Figures 5, 6 and 7 show the reception areas, of transmitter located at the origin, for all three grid patterns when K is varied from 1 to 100 with fixed $\alpha = 4.0$. The shape of reception areas, in all three grid layouts, is influenced most by the closest source of interference but as the desired minimum K increases, influence from more distant transmitters, spread around the origin, increases and shape of reception areas approaches the shape of a small circular disk with transmitter in the center.

Figure 8 shows the comparison of $\lambda\sigma_i(\lambda, K, \alpha)$ for Poisson distributed transmitters and grid arranged transmitters with varying K and fixed $\alpha = 4.0$.

2.3.2 Comparison with varying attenuation coefficient (α)

Figures 9, 10 and 11 show the variation in reception areas with increasing α.

Note that when $\alpha \to \infty$, the area of correct reception of a transmitter tends to be the Voronoi cell around this transmitter. This is because reception area is influenced most by the interference from the nearest transmitter as compared to any other transmitter. The average area of Voronoi cell equals $\frac{1}{\lambda}$. As $\alpha \to \infty$, reception area in square grid layout approaches the shape of a square with area d^2 for whatever is the K. Similarly, for hexagonal grid formation, as $\alpha \to \infty$, reception area approaches the shape of a hexagon with area $\frac{\sqrt{3}}{2}d^2$ and for honeycomb grid reception area around transmitter approaches the shape of an equilateral triangle with area $\frac{3\sqrt{3}}{4}d^2$.

Figure 12 shows the comparison of grid arranged transmitters with the case of transmitters distributed according to Poisson distribution.

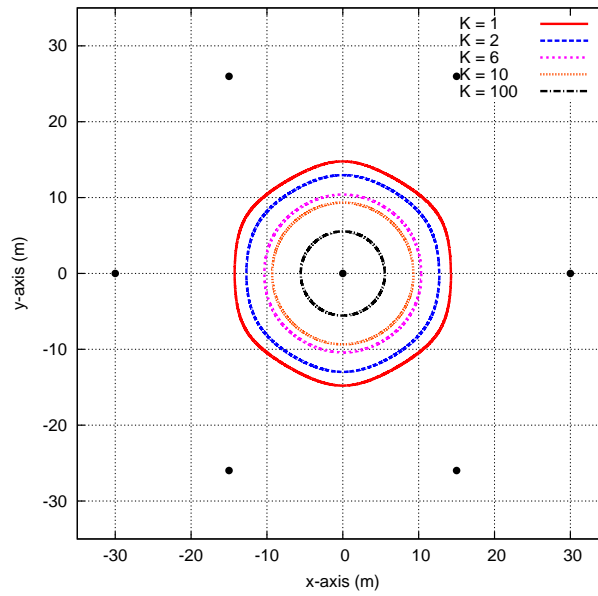For Poisson distributed transmitters, equation 3 implies that:

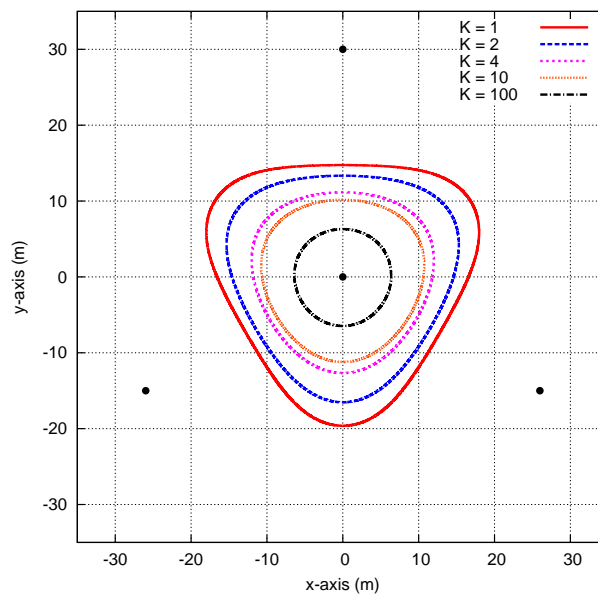Figure 6: Reception Area in Hexagonal Grid network with varying K - $d = 30m$, $\alpha = 4.0$

Figure 7: Reception Area in Honeycomb Grid network with varying K - $d = 30m$, $\alpha = 4.0$
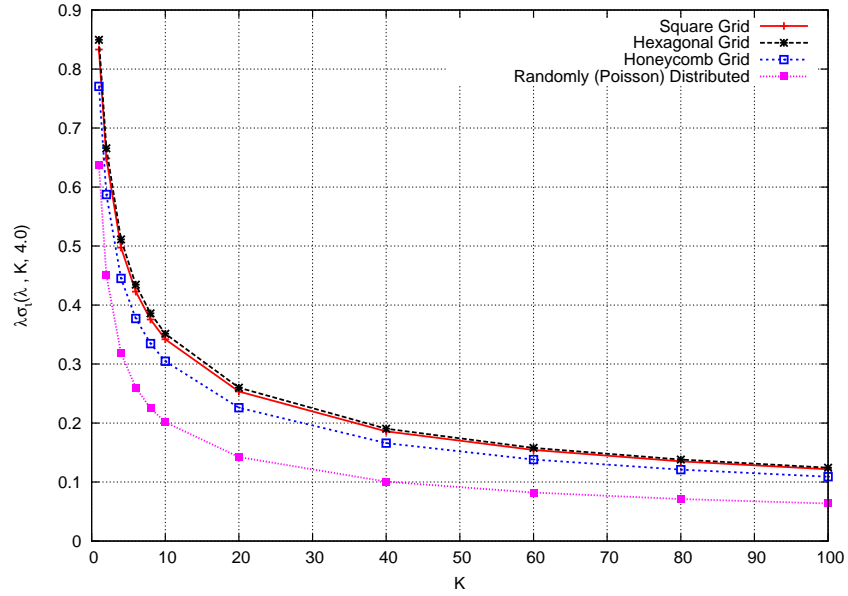
Figure 8: Comparison of Poisson distributed transmitters and Grid arranged transmitters in terms of $\lambda\sigma_i(\lambda, K, 4.0)$ with fixed $\alpha = 4.0$

$$\lim_{\alpha \to \infty} \lambda\sigma_i(\lambda, K, \infty) = 1.$$

We numerically computed $\lambda\sigma_i(\lambda, K, \alpha)$ with increasing α up to 100 and from the results, in figure 12, we can say that asymptotic result of Poisson distributed transmitters and grid arranged transmitters is same.
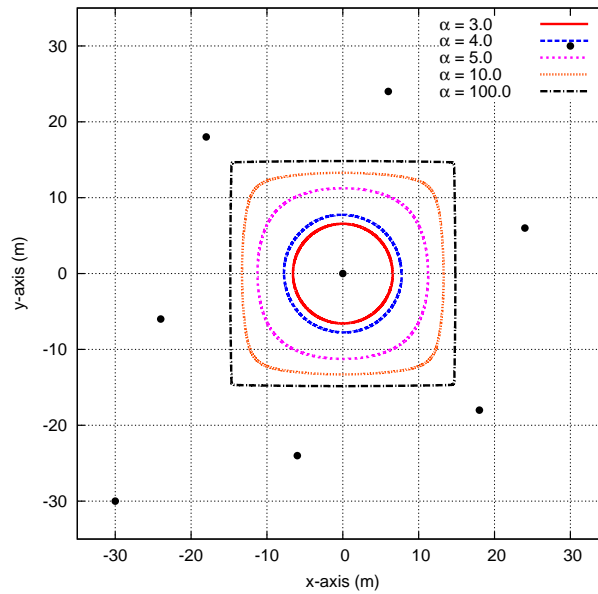
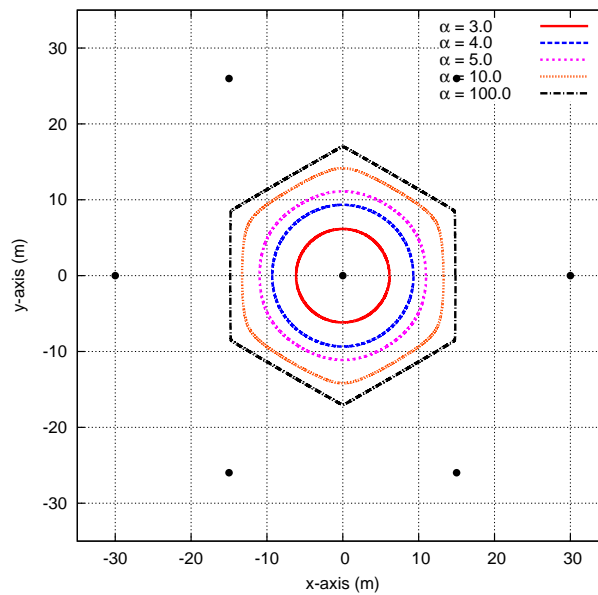Figure 9: Reception Area in Square Grid network with varying α - $d = 30m$, $K = 10.0$

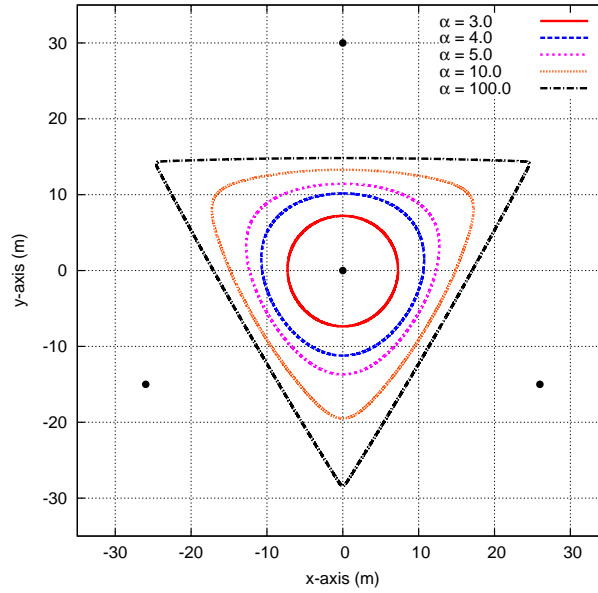Figure 10: Reception Area in Hexagonal Grid network with varying α - $d = 30m$, $K = 10.0$

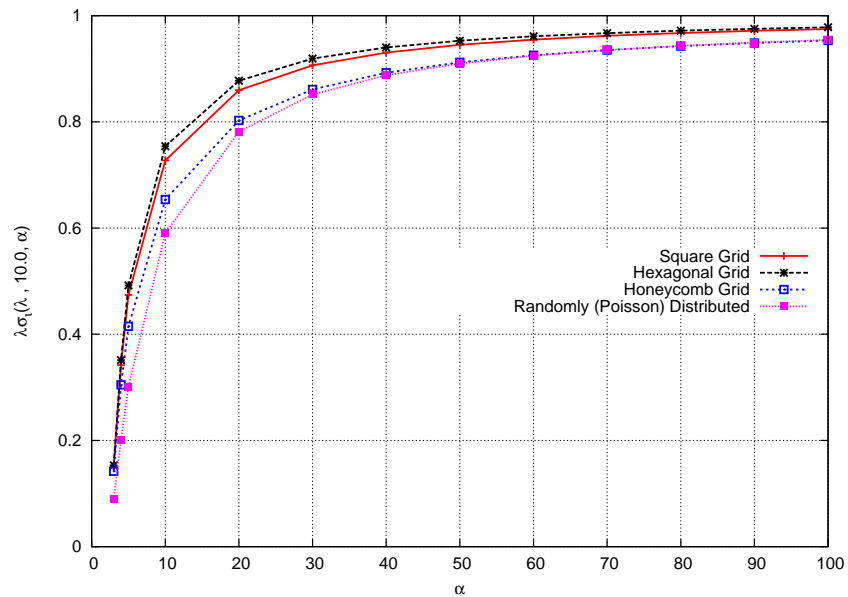Figure 11: Reception Area in Honeycomb Grid network with varying α - $d = 30m$, $K = 10.0$

Figure 12: Comparison of Poisson distributed transmitters and Grid arranged transmitters in terms of $\lambda\sigma_i(\lambda, 10.0, \alpha)$ with fixed $K = 10.0$

3   Capacity evaluation in random and grid-based networks under multi-hop configuration

Gupta and Kumar in their seminal paper characterized throughput with an asymptotic result and placed an upper bound on the throughput of multi-hop adhoc networks to be $O\left(\sqrt{\frac{N}{\log N}}\right)$ where N is the number of nodes in the network. In this section we will extend our analysis to the multi-hop case. Extending the model of previous section to evaluate the capacity in multi-hop networks is difficult. Therefore, we will develop an analytical model for computing throughput of a wireless network under multi-hop configuration.

In one of the first papers on throughput in multi-hop networks, [11] analyzed slotted ALOHA protocol and showed that the critical performance parameter is p - probability of transmission in any time-slot.

The authors of [2] developed an analytical model of slotted ALOHA in multi-hop networks and showed that transport capacity can be optimized by selecting an appropriate value of p.

[9] investigated the single-hop and multi-hop throughput using slotted ALOHA protocol and analyzed the Performance Accident when multi-hop throughput reaches the single-hop throughput and optimal probability of channel access - p - shifts dramatically from $\frac{1}{N}$ to $\frac{1}{\log N}$.

We will use our analytical model with simulator to compare maximum throughput that can be achieved in a network under Constrained TDMA, Constrained Grid TDMA and simple ALOHA-based protocols. We will describe the model of Constrained TDMA and Constrained Grid TDMA protocols later in section 3.1.2.

This section is organized as follows. In section 3.1 we present the details of the network model we have used. Analytical model for computing throughput in a network is discussed in the section 3.2. Section 3.3 gives detail of our simulation methodology and results from comparison of different protocols can be found in the section 3.4. We performed experiments for:

- Comparison of slotted ALOHA and Constrained TDMA

- Comparison of Constrained TDMA and Constrained Grid TDMA

3.1   System model

Following are the major assumptions of our model.

3.1.1   Physical model

We have used the same physical model as was used in section 2.
   Details of this model are:

- All transmitting nodes have the same unit nominal transmission power.

- The signal received at distance r from the transmitter is $\frac{1}{r^\alpha}$. We have assumed $\alpha = 4.0$.

- A packet is correctly received if its SNR is greater or at least equal to K where noise is the sum of the signal powers received from all others

transmitters, acting as sources of interference, in the same time-slot. This is identical to the SNR model used in section 2 in equation 1:

$$\frac{|z - z_i|^{-\alpha}}{\sum\limits_{j \neq i} |z - z_j|^{-\alpha}} \geq K$$

3.1.2 Protocol models

- The time is slotted.

- In slotted ALOHA access protocol every node transmits a packet on any given slot with probability p, independently of the other nodes.

- In our analysis we do not consider any particular TDMA-based protocol. We only assume that same time-slot shall not be used within a certain neighborhood and refer to the protocols following this reservation rule as constrained TDMA protocols. The radius of this neighborhood is defined in terms of two parameters: m representing the number of hops and r representing the distance of 1-hop in euclidean space (such that all nodes lying at distance less than r are at 1-hop). Therefore a time slot cannot be shared within a distance of less than $m.r$ or, in other words, nodes transmitting in the same slot shall be located at a distance greater or equal to $m.r$ from each other.

In this study we consider the following two types of constrained TDMA protocols:

1. Constrained TDMA

   In Constrained TDMA protocol, the list of simultaneously transmitting nodes is built by random draws while following the above specified reservation rule for channel access. This is similar to the TDMA model use in [3]. The set of transmitters $\mathcal{S}$ which are transmitting in the same time slot is built as follows:

   (a) Initialize: $\mathcal{N} = \{s_1, s_2, ..., s_N\}$ and $\mathcal{S} = \emptyset$.
   (b) Randomly select a node s_i from $\mathcal{N}$ and add it to the set $\mathcal{S}$: $\mathcal{S} := \mathcal{S} \cup \{s_i\}$.
   (c) Remove s_i from the set $\mathcal{N}$.
   (d) Remove all nodes from the set $\mathcal{N}$ which are at distance less than $m.r$ from s_i.
   (e) If set $\mathcal{N}$ is non-empty, repeat from step (c).

2. Constrained Grid TDMA

   In Constrained Grid TDMA protocol, the nodes which transmit simultaneously in a time slot form a specific grid pattern. The dimension d of this grid pattern is related to the parameters, m and r, as:

$$d = m.r$$

   Figure 3 shows the realization of square, hexagonal and honeycomb grid patterns from dimension d.

In section 2 we have shown that hexagonal grid pattern gives the maximum local capacity i.e. the information rate received by an arbitrarily placed node. Using the hypothesis that maximum local capacity will also result in maximum multi-hop capacity[1], in this section we will evaluate the hexagonal grid pattern only.

The set of transmitters $\mathcal{S}$ is built as follows.

(a) Initialize: $\mathcal{N} = \{s_1, s_2, ..., s_N\}$ and $\mathcal{S} = \emptyset$.

(b) Randomly select a node s_i from $\mathcal{N}$ and add it to the set $\mathcal{S}$: $\mathcal{S} := \mathcal{S} \cup \{s_i\}$.

(c) Construct a virtual hexagonal grid, from the position of s_i, with dimension d.

(d) All nodes which overlap with the points of virtual hexagonal grid will be added to the set $\mathcal{S}$.

3.1.3 Traffic model

- The network throughput is computed under the assumption that traffic model is uniform and every node sends equal traffic to every other node in the network.

- We assume that every node has an infinite transmit buffer filled with packets (since we want to compute the ultimate throughput).

3.1.4 Network map

The network map is a square area $\mathcal{A} = 100 \times 100m^2$ with N nodes distributed over it.

3.2 Throughput computation

Here we will present the analytical model for computing throughput of the network in terms of packets per time-slot.

The goal of the simulation run with N nodes can be limited to the measurement of the Average Reception Matrix. The average reception matrix C is the matrix whose coefficient: c_{ij} represents the proportion of transmissions from node i which are successfully received by node j.

The average number of retransmissions, including the first transmission, required for delivering a packet from node i to node j will be $\frac{1}{c_{ij}}$. Let us call the matrix $\frac{1}{c_{ij}}$ the transmission cost matrix D_{ij} where $D_{ij} = \frac{1}{c_{ij}}$ (we set $D_{ii} = 0$ for all i). Therefore the average number of retransmissions needed to deliver a packet from node i to node j is D_{ij}.

Each node i computes its best route to any destination j by performing Dijkstra algorithm on the matrix D. The best route is the route $(i_1, i_2, ..., i_k)$ such that $i_1 = i$ and $i_k = j$ and $\sum D_{i_l} D_{i_{l+1}}$ is minimal. Let M_{ij} be this minimal value and it will represent the minimum optimal number of retransmissions from node i to node j. We use the $(\min, +)$ algorithm to compute the min hop matrix M. We set $M = D$ and iterate $M \leftarrow M * D$ until M is stationary,

---

[1]This can be verified using the simulation model we have developed in this section.

with $(M * D)_{ij} = \min_l(M_{il} + D_{lj})$. There could be only a maximum of $\log N$ iterations.

Let R_i be the traffic rate of node i and it is equal to the proportion of slots when node i is active. In case of slotted ALOHA, R_i should be equal to the probability of medium access, p.

During T slots, there are on average $T \sum R_i$ packet transmission attempts in the network. If ρ is the throughput of the system in packets per time-slot, the number of successfully delivered packets is ρT. Since each node sends equal traffic to every other node and there are $N(N-1)$ pairs of source and destination, the number of packets delivered from source i to destination j during T slots is $\frac{\rho T}{N(N-1)}$.

The transmission cost from source i to destination j is M_{ij}, therefore $\rho \frac{\sum\limits_{i,j} M_{ij}}{N(N-1)} T$ is equal to the average number of transmission attempts in the network during T slots and should be equal to $T \sum R_i$. Therefore, throughput of the network is:

$$\rho = \frac{N(N-1) \sum R_i}{\sum\limits_{i,j} M_{ij}}$$

In case of slotted ALOHA, $\sum R_i = pN$ and net throughput expression reduces to: $\rho = \frac{N^2 p (N-1)}{\sum\limits_{i,j} M_{ij}}$ which is similar to the analytic expression, derived in [9], for throughput with slotted ALOHA protocol.

3.3 Simulation technique

We have used two different schemes for distribution of N nodes in the network area $\mathcal{A}$. In the first scheme, N nodes are dispatched in the network area according to Poisson distribution and throughput of this network is computed with slotted ALOHA and Constrained TDMA medium access protocols.

Poisson distributed nodes may not give the maximum throughput with Constrained Grid TDMA protocol especially at low network densities. At lower network densities, many points of virtual grid, constructed from any randomly selected node, may not overlap with any other node and hence the number of active transmitters in the network, in any given slot, will be lower than the optimal number possible within the constraints of Constrained Grid TDMA protocol. Since we are interested in finding the ultimate throughput, we have devised another scheme for dispatching nodes in the network area $\mathcal{A}$.
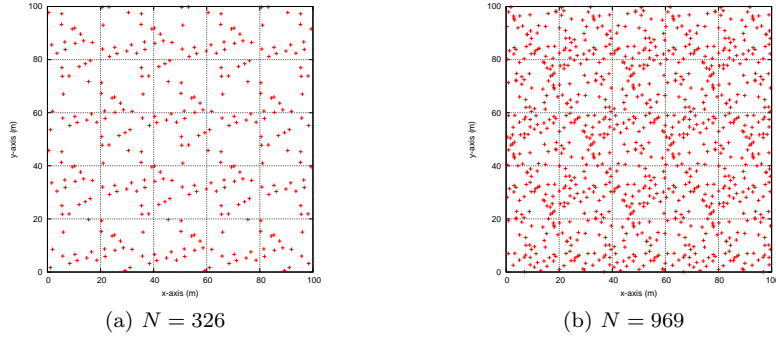
(a) $N = 326$ (b) $N = 969$

Figure 13: Location distribution of N nodes on 100 x $100m^2$ area using grid based distribution scheme

Consider a hexagonal grid pattern spread over an infinite area also containing the network area $\mathcal{A}$. Depending on d, let's say maximum n number of nodes will lie within $\mathcal{A}$. We may call this hexagonal grid pattern, with n nodes in $\mathcal{A}$, a grid frame.

There shall be at least $\frac{N}{n}$ such grid frames, with each frame contributing a maximum of n nodes to the network, in order to have N nodes in $\mathcal{A}$.

All these grid frames shall be superimposed over each other such that each frame is displaced along $x-$ and $y-$axes. This displacement is uniformly selected from the interval $[-2d, +2d]$.

Figure 13 shows the distribution of 326 and 969 nodes in the network area of 100 x $100m^2$ with $d = m.r = 30m$ ($m = 2, d = 15m$). Note that at lower network densities, there will be fewer grid frames and clustering of nodes can be observed but as the network density increases, nodes appear well spread over the network area.

The average reception matrix C is computed via simulation of packet transmissions. Each node, when transmitting, sends out a broadcast packet in the network and, from SNR model, we can compute the coefficients c_{ij} of the matrix C. Note that in case of Constrained Grid TDMA protocol, the received signal and interference levels, for the source and destination pair (i, j), remains constant and c_{ij} is computed numerically.

3.4 Results

The transmission probability and number of nodes in the network are varied in order to understand the nature of throughput w.r.t. these parameters. Note that in case of constrained TDMA based protocols, transmission probability implicitly depends on m. Therefore for constrained TDMA based protocols we will vary m and investigate its effect on the network throughput.

3.4.1 Slotted ALOHA and Constrained TDMA protocols

We know that the single-hop throughput in a network with slotted ALOHA protocol is $\rho_s \geq pN(1-p)^{N-1}$. Therefore an optimal value of p is $\approx \frac{1}{N}$ which

would give $\rho_s \approx \frac{1}{e}$. Note that single-hop throughput is slightly higher than $\frac{1}{e}$ because of the spatial reuse in the network when more than one simultaneous transmissions can be successful. Since single-hop communication is a special case of multi-hop communication, multi-hop throughput $\rho_m \geq \rho_s$. Gupta and Kumar in [6] placed an upper bound on the throughput of multi-hop adhoc networks in the order of $\sqrt{\frac{N}{\log N}}$. To achieve this asymptotic behavior, we expect to get maximum throughput with p of the order of $\frac{1}{\log N}$ when N is large.

Figure 14 shows the throughput achieved with slotted ALOHA protocol in network with N Poisson distributed nodes. It can be observed that throughput increases initially, followed by a decrease and then an increase with rate in the order of $\sqrt{N}$. The first local maxima observed at $p \approx \frac{1}{N}$ occurs because of the single-hop nature of the transmissions. This accounts for the initial increase and subsequent decrease in throughput. As the number of nodes in the network increase, a second maxima starts to develop. This second maxima increases with increasing number of nodes and occurs at $p \approx \frac{c}{\log N}$ where $c \approx 0.25$. Flat nature of the curvature at second maxima makes it difficult to get the accurate value of c. The dramatic shift of optimal value of p from $\frac{1}{N}$ to $\frac{c}{\log N}$ is called performance accident and it can be observed easily in figure 15 when optimal value of p shifts dramatically for $N \approx 113$. Performance accident is studied in detail in [9].
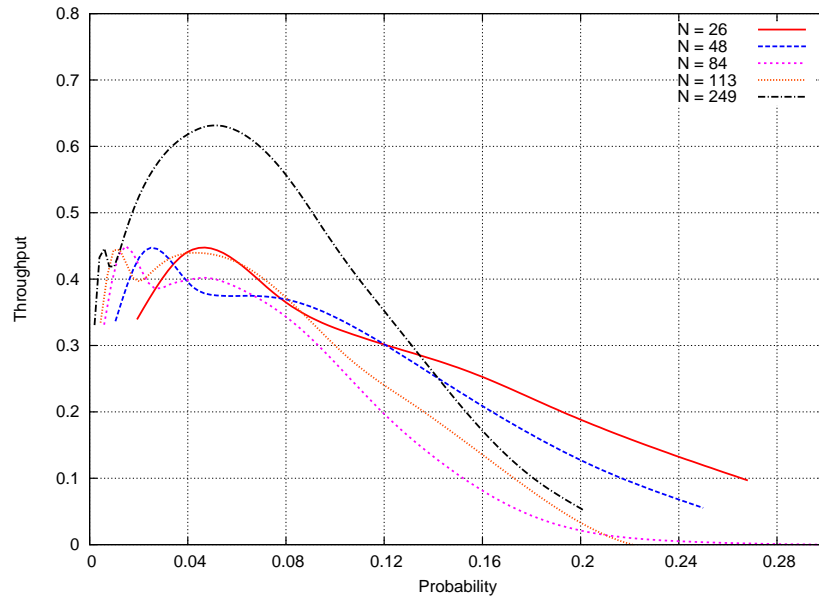

Figure 14: Throughput with slotted ALOHA protocol. Nodes are dispatched in network area of 100 x 100m^2 according to Poisson distribution.
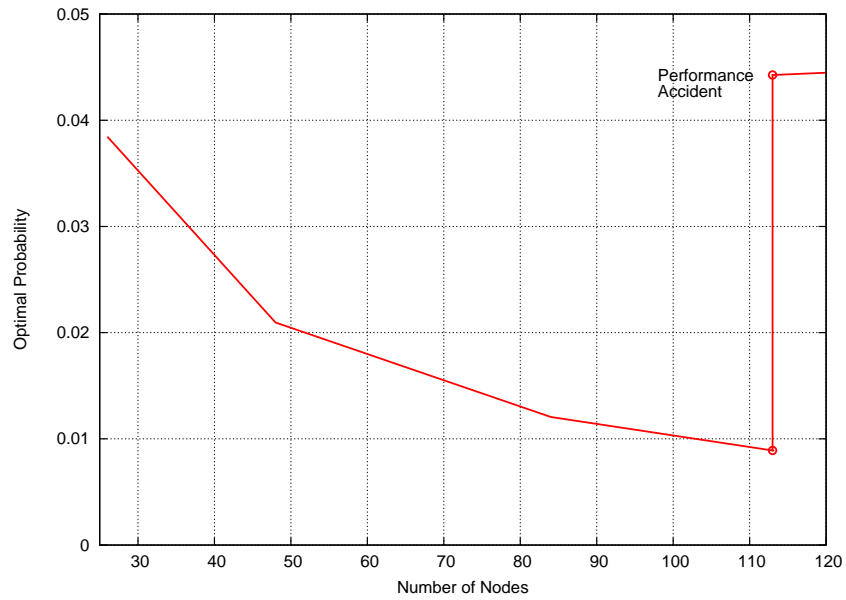
Figure 15: Optimal Probability of Transmission vs. Number of Nodes. Nodes are dispatched in network area of 100 x $100m^2$ according to Poisson distribution.
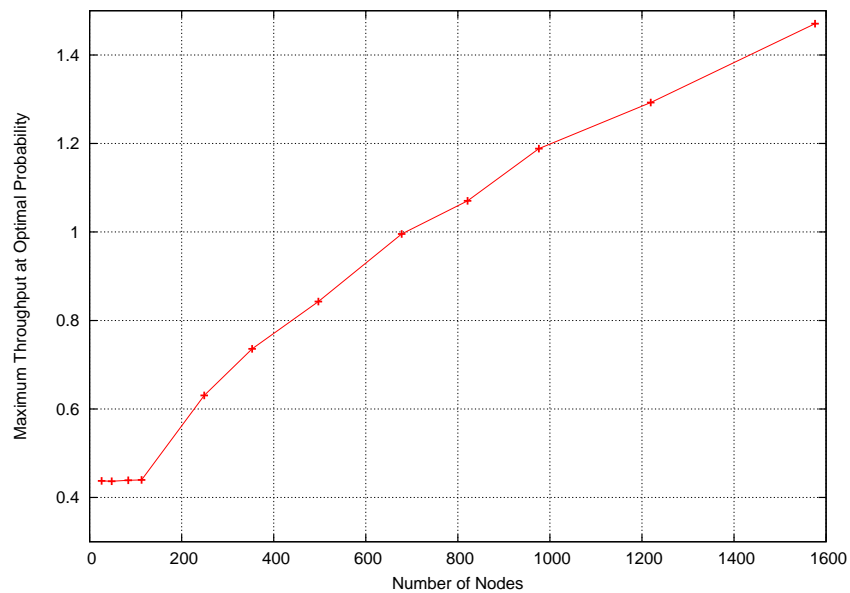

Figure 16: Throughput at optimal p with slotted ALOHA protocol. Nodes are dispatched in network area of 100 x $100m^2$ according to Poisson distribution.
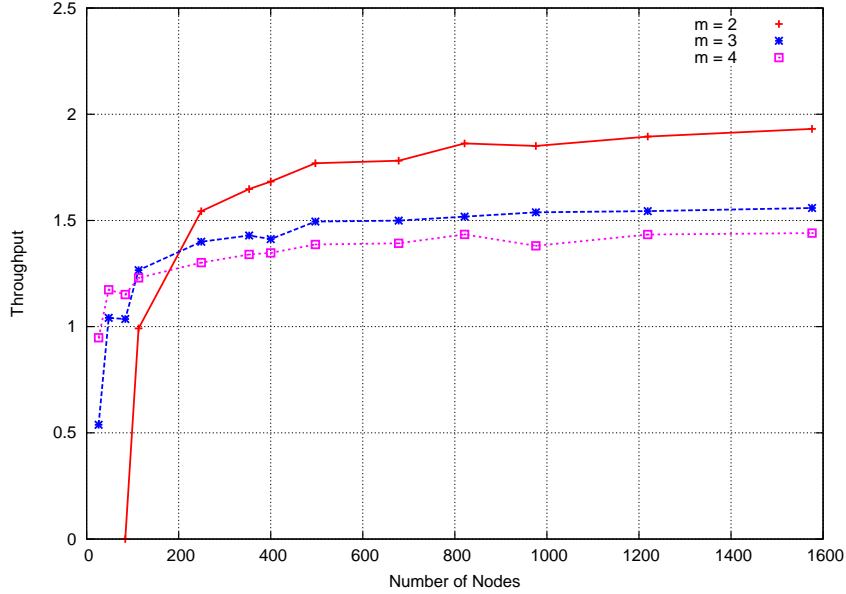
Figure 17: Throughput with Constrained TDMA protocol with varying m. Parameters: $r = 15m$ and $d = m.r$. Nodes are dispatched in network area of 100 x $100m^2$ according to Poisson distribution

Figure 16 shows the maximum throughput achieved by slotted ALOHA protocol with optimal value of p. Note that before the occurrence of performance accident, maximum throughput remains constant at a value slightly higher than $\frac{1}{e}$. This almost constant maximum throughput can be explained by the single-hop nature of the transmissions. As the number of nodes in the network increase, the multi-hop throughput out-performs the single-hop throughput.

For Constrained TDMA protocol, we have set $r = 15m$ and m is varied from 2 to 4. Under these conditions, the nodes transmitting simultaneously will be at least at a distance of $d = m.r$ from each other. Figure 17 shows throughput in the same network with Constrained TDMA protocol. It can be observed that at very low network densities, throughput with $m = 3$ or $m = 4$ is higher than the throughput with $m = 2$. The reason can be the sparsely located nodes and higher number of active transmitters with $m = 2$. This may reduce the number of available intermediate nodes required for multi-hop communication from source to destination but as the network density increases, throughput with $m = 2$ out-performs throughput with higher values of m.

3.4.2 Constrained TDMA and Constrained Grid TDMA protocols

For comparing Constrained TDMA protocol with Constrained Grid TDMA protocol we have used the grid based distribution of nodes. We have set $r = 15m$ and $m = 2$. Each grid frame is therefore constructed with the dimension $d = m.r = 30m$.
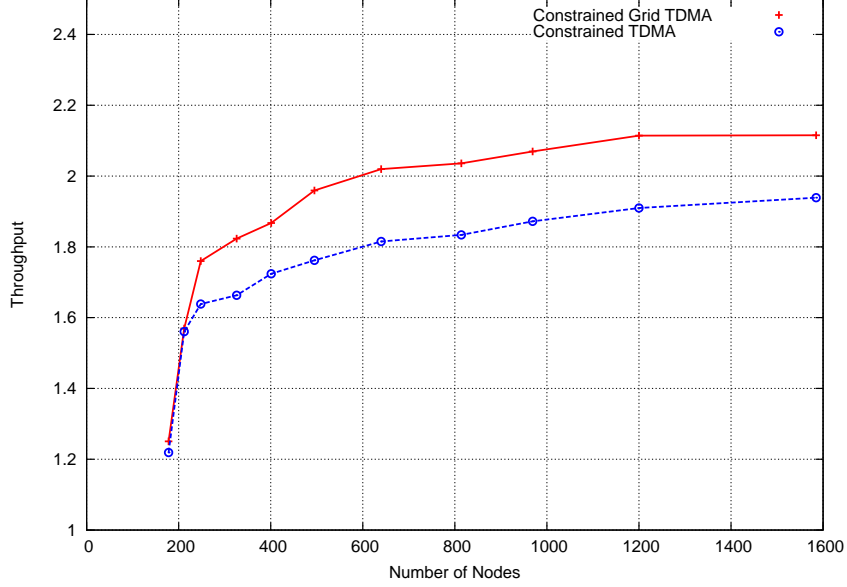
Figure 18: Throughput comparison of Constrained TDMA and Constrained Grid TDMA protocols. Parameters: $m = 2$, $r = 15m$ and $d = m.r = 30m$. Nodes are spread over an area of $100.100m^2$ based on grid based distribution

Note that as the node density increases, throughput of Constrained Grid TDMA protocol is observed to be slightly higher than the typical Constrained TDMA protocol. This can be explained by the corresponding increase in the average density of successful receivers in the coverage area of any transmitter resulting in higher local capacity, $\lambda\sigma(\lambda, K, \alpha)$, in grid based networks. This result also verifies our hypothesis that higher local capacity in grid based networks will result in higher multi-hop capacity.

4　Field optimization for wireless capacity

Consider an infinite set of points $S = \{z_1, z_2, \ldots, z_n, \ldots\}$ on the plane. We denote $x_i(z) = \frac{|z-z_i|^{-\alpha}}{\sum_j |z-z_j|^{-\alpha}}$. Let $\alpha > 2$. In order to simplify notations, we will remove the reference to z when no ambiguity is possible. We define a function $f(x_i)$ which can be continuous or integrable. For instance we will use $f(x_i) = 1_{x_i > K}$ for some given K.

We suppose that the set density $\nu(S)$ has a limit:

$$\nu(S) = \lim_{R \to \infty} \frac{1}{\pi R^2} \sum_i 1_{|z_i| \leq R} \ .$$

We denote $h(z) = \sum_i f(x_i)$ and we want to optimize $\mathbf{E}(h(z))$ defined by the limit:

$$\mathbf{E}(h(z)) = \lim_{R \to \infty} \frac{1}{\pi R^2} \int_{|z| \leq R} h(z) dz^2 \ .$$

We denote $\sigma_i = \int f(x_i) dz^2$ and we have

$$\mathbf{E}(h(z)) = \lim_{R \to \infty} \frac{1}{\pi R^2} \sum_i 1_{|z_i| \leq R} \sigma_i = \nu(S) \mathbf{E}(\sigma_i)$$

with

$$\mathbf{E}(\sigma_i) = \lim_{n \to \infty} \frac{1}{n} \sum_{i \leq n} \sigma_i \ .$$

We denote ∇_i the operator of differentiation with respect to z_i.

We have for $i \neq j$:

$$\nabla_i x_j = \alpha x_i x_j \frac{z - z_i}{|z - z_i|^2}$$

and

$$\nabla_i x_i = \alpha (x_i^2 - x_i) \frac{z - z_i}{|z - z_i|^2} \ .$$

Therefore,

$$\nabla_i h(z) = \alpha x_i \frac{z - z_i}{|z - z_i|^2} \left(-f'(x_i) + \sum_j x_j f'(x_j) \right) \ .$$

Although $\int h(z) dz^2 = \infty$, we nevertheless have a finite $\nabla_i \int h(z) dz^2$. In other words, the sum $\sum_j \nabla_i \sigma_j$ converges for all i.

We also know that for all j in S, $\sum_i \nabla_i \sigma_j = 0$. Indeed this would be the differentiation of σ_j when all points in S are translated by the same vector. Similarly $\sum_i \nabla_i \int h(z) dz^2 = 0$.

If S is a grid, then: $\nabla_i \int h(z) dz^2 = \sum_j \nabla_i \sigma_j$ and therefore would be null (since $\sum_i \nabla_i \int h(z) dz^2 = 0$).

We could conclude erroneously that:

- all grid sets are optimal;

- all grid sets give the same $\mathbf{E}(h(z))$.

In fact this is wrong: we could also conclude that $\mathbf{E}(\sigma_i)$ does not vary but this will contradict that $\nu(S)$ *must* vary. The reason of this error is that a grid set cannot be modified into another grid set with uniformly bounded transformation, unless the two grid sets are just simply translated by a simple vector.

However we prove that the grid sets are *locally* optimal within sets that can be uniformly transformed between each other.

In order to cope with uniform transformation and to be able to transform a grid set to another grid set we introduce the linear group transformation. We only consider the grid situation, therefore:

$$\mathbf{E}(h(z)) = \sigma_0 = \int f(x_0) dz^2 \ .$$

4.1 Linear group transformation

Here we assume that the points in z are modified according to a continuous linear transform $M(t)$ where $\mathbf{M}(t)$ is a matrix with $\mathbf{M}(0) = \mathrm{I}$, for example $\mathbf{M}(t) = \mathrm{I} + t\mathbf{A}$ with $\mathbf{A}$ a matrix. Under this assumption we have

$$\frac{\partial}{\partial t}\sigma_0 = \sum_i (\mathbf{A}z_i.\nabla_i\sigma_0)$$

Therefore the derivative of σ_0 with respect to matrix $\mathbf{A}$ is $\sum_i \mathbf{A}z_i.\nabla_i\sigma_0 = \mathrm{tr}(\mathbf{A}(\sum_i z_i \otimes \nabla_i\sigma_0))$. In other words the derivative with respect to matrix is exactly $\mathbf{D} = \sum_i z_i \otimes \nabla_i\sigma_0$.

$$\mathbf{D} = \left[\begin{array}{cc} D_{xx} & D_{xy} \\ D_{yx} & D_{yy} \end{array} \right]$$

Let assume that $\mathbf{M}(t) = (1+t)\mathrm{I}$, *i.e.* the linear transform is homothetic. In this case we have $\sigma_0(t) = (1+t)^2\sigma_0$ and $\mathbf{A} = \mathrm{I}$. As a first property we have $\mathrm{tr}(\mathbf{D}) = 2\sigma_0$ since the derivative of σ_0 with respect to identity matrix I is exactly $2\sigma_0$ (since $\sigma_0'(0) = 2\sigma_0$). Less obvious is the fact that $\mathbf{D}$ is a symmetric matrix. The easiest proof of this property is to consider the derivative with respect to matrix J:

$$\mathrm{J} = \left[\begin{array}{cc} 0 & -1 \\ 1 & 0 \end{array} \right]$$

which is zero since J is the initial derivative for a rotation. Since $\mathrm{tr}(\mathbf{J}\mathbf{D}) = D_{yx} - D_{xy}$, this implies that $\mathbf{D}$ is symmetric.

Let $\mathbf{T}$ be defined as:

$$\mathbf{T} = \int dz^2 \sum_i (z - z_i) \otimes \nabla_i f(x_0) \ .$$

The sum $\sum_i (z - z_i) \otimes \nabla_i f(x_0)$ leads to a symmetric matrix since

$$\mathbf{T} = \alpha \int f'(x_0)$$
$$\times \left(\frac{x_0^2 - x_0}{\|z - z_0\|^2}(z - z_0) \otimes (z - z_0) + \sum_{i \neq 0} \frac{x_0 x_i}{\|z - z_i\|^2}(z - z_i) \otimes (z - z_i) \right) dz^2$$

and the left hand side is made of $(z - z_i) \otimes (z - z_i)$ that are symmetric matrices.

Since,

$$\begin{aligned} \mathbf{D} &= \sum_i z_i \otimes \nabla_i\sigma_0 \\ &= \int dz^2 \sum_i z_i \otimes \nabla_i f(x_0) \end{aligned}$$

we have

$$\mathbf{D} + \mathbf{T} = \int dz^2 \sum_i z \otimes \nabla_i f(x_0)$$

It remains to prove that $\int \sum_i z \otimes \nabla_i f(x_0) dz^2$ is symmetric too. Since

$$\sum_i \nabla_i f(x_0) = -\nabla f(x_0)$$

we have

$$\int \sum_i z \otimes \nabla_i f(x_0) dz^2 = - \begin{bmatrix} \int x \frac{\partial}{\partial x} f(x_0) dx dy & \int x \frac{\partial}{\partial y} f(x_0) dx dy \\ \int y \frac{\partial}{\partial x} f(x_0) dx dy & \int y \frac{\partial}{\partial y} f(x_0) dx dy \end{bmatrix}$$

$$= \begin{bmatrix} \sigma_0 & 0 \\ 0 & \sigma_0 \end{bmatrix} = \sigma_0 \mathbf{I}$$

which is symmetric.

We know that $\mathbf{T}$ is symmetric and $\mathbf{D} + \mathbf{T} = \sigma_0 \mathbf{I}$. Thus $\mathrm{tr}(\mathbf{T}) = 0$

When grid is optimal, we must have $\mathbf{T} = 0$. In any case, the matrix $\mathbf{T}$ must be invariant with respect to isometric symmetries of the grid. For the square grid, we have all symmetries with respect to any horizontal or vertical axes of the grid and in particular with the rotation of $\frac{\pi}{2}$ represented by J. Therefore the Eigen system must be invariant by rotation of $\frac{\pi}{2}$. This implies that the eigenvalues are the same and therefore null since $\mathrm{tr}(\mathbf{T}) = 0$.

Same argument for the hexagonal grid, with the invariance for $\frac{\pi}{3}$ rotation and for the honeycomb pattern with invariance in $\frac{\pi}{6}$ rotation. In both cases $\mathbf{T} = 0$.

Of course this does not exclude other grids or patterns with $\mathbf{T} = 0^2$.

---

[2]This remains to be proven.

Appendix

(a) Computation of $\nabla S_i(z)$

From equation 6
$$S_i(z) = \frac{|z-z_i|^{-\alpha}}{\sum\limits_{j\neq i}|z-z_j|^{-\alpha}} = \frac{f}{g}$$

where,
$$f = |z-z_i|^{-\alpha} \text{ and } g = \sum\limits_{j\neq i}|z-z_i|^{-\alpha}.$$

Let $r_i = |z-z_i|$ and $r_j = |z-z_j|$. The gradients of f and g will be:

$$\nabla f = -\alpha|z-z_i|^{-\alpha-1}\frac{z-z_i}{|z-z_i|} = -\alpha\frac{1}{r_i^{\alpha+1}}\frac{z-z_i}{r_i}$$

$$= -\alpha\frac{z-z_i}{r_i^{\alpha+2}}$$

$$\nabla g = \sum\limits_{j\neq i} -\alpha\frac{z-z_j}{r_j^{\alpha+2}}$$

Using identity
$\nabla\frac{f}{g} = \frac{1}{g^2}(g\nabla f - f\nabla g)$, we get

$$
\begin{aligned}
\nabla S_i(z) &= \begin{bmatrix} \frac{\partial}{\partial x}S_i(z) \\ \frac{\partial}{\partial y}S_i(z) \end{bmatrix} \\
&= \begin{bmatrix} \frac{1}{\left(\sum\limits_{j\neq i}r_j^{-\alpha}\right)}\left((\sum\limits_{j\neq i}r_j^{-\alpha})(-\alpha\frac{x-x_i}{r_i^{\alpha+2}}) - (r_i^{-\alpha})(\sum\limits_{j\neq i}-\alpha\frac{x-x_j}{r_j^{\alpha+2}})\right) \\ \frac{1}{\left(\sum\limits_{j\neq i}r_j^{-\alpha}\right)}\left((\sum\limits_{j\neq i}r_j^{-\alpha})(-\alpha\frac{y-y_i}{r_i^{\alpha+2}}) - (r_i^{-\alpha})(\sum\limits_{j\neq i}-\alpha\frac{y-y_j}{r_j^{\alpha+2}})\right) \end{bmatrix}
\end{aligned}
$$

(b) Locating the starting point z on closed curve bounding reception area

The SNR $S_i(z)$ at point z should be greater or at least equal to K. We assume that it is equal to K. Then using equation 6

$$\frac{|z-z_i|}{\sum\limits_{j\neq i}|z-z_j|} = K$$

Our aim is to find the coordinates of point z which satisfy above relation. To simplify computation of point z on the closed curve, bounding reception area of transmitter i located at $z_i = (x_i, y_i)$, its y coordinate can be fixed such that $z = (x, y) = (x, y_i)$. This reduces the SNR equation to

$$\frac{|x - x_i|}{\sum\limits_{j\neq i}|z - z_j|} - K = 0 \tag{8}$$

Equation 8 is a function of variable x and can be solved using Newton's Method.

Remark: Newton's Method: Given a function $f(x)$ and its derivative $f'(x)$ begin with a first guess x_0. Provided the function is reasonably well-behaved a better approximation x_1 is $:= x_0 - \frac{f(x_0)}{f'(x_0)}$. The process is repeated until a sufficiently accurate value is reached:

$$x_{n+1} = x_n - \frac{f(x_n)}{f'(x_n)} \tag{9}$$

From 8,
$f(x) = \frac{|x-x_i|^{-\alpha}}{\sum\limits_{j\neq i}|z-z_j|^{-\alpha}} - K$
Assume,
$g = r_i^{-\alpha}$ and $h = \sum\limits_{j\neq i} r_j^{-\alpha}$
where,
$r_i = |x - x_i|$ and
$r_j = |z - z_j|$.
Newton's Method requires the derivative of $f(x)$ which is computed as below.
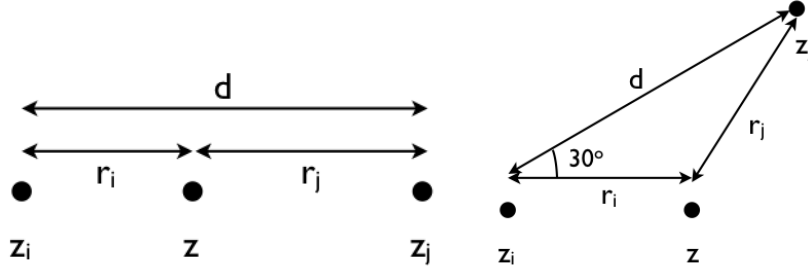$\frac{d}{dx}g = -\alpha\frac{x-x_i}{r_i^{\alpha+2}}$
$\frac{d}{dx}h = \sum\limits_{j\neq i} -\alpha\frac{z-z_j}{r_j^{\alpha+2}}$
The first derivative of the function $f(x)$ is,

$$f'(x) = \frac{1}{h^2}(h\frac{d}{dx}g - g\frac{d}{dx}h)$$

$$= \frac{1}{\left[\sum\limits_{j\neq i}r_j^{-\alpha}\right]}\left[(\sum\limits_{j\neq i}r_j^{-\alpha})(-\alpha\frac{x-x_i}{r_i^{\alpha+2}}) - (r_i^{-\alpha})(-\alpha\frac{z-z_j}{r_j^{\alpha+2}})\right]$$

Newton's Method also requires first approximation of the root, x_0. An approximate value, closer to the actual root, can significantly reduce the number of iterations in Newton's Method.

(a) In case of square and hexagonal grid networks (b) In case of honeycomb grid network

Figure 19: Geometric representation of finding the first approximation of point $z = (x_0, y_i)$

In all three types of grid networks, the transmitter closest to i, hereafter referred to as j, lies at distance d and hence can give the best estimate x_0. For first approximation x_0, we can ignore all other transmitters in the network. In this case,

$$\frac{|z - z_i|^{-\alpha}}{|z - z_j|^{-\alpha}} \geq K$$

$$\frac{r_i^{-\alpha}}{r_j^{-\alpha}} \geq K : i \neq j$$

where $r_i = |z - z_i|$ and $r_j = |z - z_j|$.

$$\frac{r_j}{r_i} \leq (K)^{\frac{1}{\alpha}}$$

The location of transmitters i and j and point z in the plane form three corners of a triangle with angle (θ) equal to 0 in case of square and hexagonal grid and 30 degrees is case of honeycomb grid layout. Figure 19 shows the location of transmitters z_i and z_j, point z and distances r_i, r_j and d. Using above relation between r_i and r_j and Law of Cosines, we get the solution of r_i as

$r_i = \frac{-B \pm \sqrt{B^2 - 4AC}}{2A}$
where
$A = 1 - K^{\frac{2}{\alpha}}$
$B = -2.d.cos(\theta)$ and
$C = d^2$.

d is the distance between transmitters i and j and is known parameter of the grid layout.

> *Remark: Select positive value of r_i as the solution of the above quadratic equation. Using $x_0 = x_i + r_i$ as the first approximate solution in Newton's Method (equation 9), and after a few iterations, we can get a sufficiently accurate value x_{n+1} which will be the x coordinate of the point z.*

The coordinates of point z will be: (x_{n+1}, y_i).

References

[1] François Baccelli and Bartek Blaszczyszyn. On a Coverage Process Ranging from the Boolean Model to the Poisson Voronoi Tessellation With Applications to Wireless Communications. 0 RR-4019, INRIA, 10 2000. Projet MCR.

[2] François Baccelli, Bartlomiej Blaszczyszyn, and Paul Muhlethaler. An aloha protocol for multihop mobile wireless networks. *IEEE Transactions on Information Theory*, 52:421–436, 2006.

[3] Skander Banaouas and Paul Muhlethaler. Performance evaluation of tdma versus csma-based protocols in sinr models. In *European Wireless*, 2009.

[4] Lichun Bao and J.J. Garcia-Luna-Aceves. A new approach to channel access scheduling for ad hoc networks. In *Proc. ACM Seventh Annual International Conference on Mobile Computing and networking*, pages 210–221, 2001.

[5] Shashidhar Gandham. Link scheduling in sensor networks: Distributed edge coloring revisited. In *INFOCOM*, pages 2492–2501, 2005.

[6] Piyush Gupta, Student Member, and P. R. Kumar. The capacity of wireless networks. *IEEE Transactions on Information Theory*, 46:388–404, 2000.

[7] Kezhu Hong and Yingbo Hua. Throughput analysis of large wireless networks with regular topologies. *EURASIP J. Wirel. Commun. Netw.*, 2007(1):3–3, 2007.

[8] P. Jacquet. Shannon capacity in poisson wireless network model. *Probl. Inf. Transm.*, 45(3):193–203, 2009.

[9] Philippe Jacquet and Prateek Mittal. The Performance Accident in wireless multi-hop networks. Research Report RR-5746, INRIA, 2005.

[10] Xiaowen Liu and Martin Haenggi. Throughput analysis of fading sensor networks with regular and random topologies. *EURASIP J. Wirel. Commun. Netw.*, 2005(4):554–564, 2005.

[11] Randolph Nelson and Leonard Kleinrock. The spatial capacity of slotted aloha multihop packet radio network with capture. *IEEE Transactions on Communications*, Vol.Com 32(No-6), June 1984.

[12] Injong Rhee, Ajit Warrier, Jeongki Min, and Lisong Xu. Drand: distributed randomized tdma scheduling for wireless ad-hoc networks. In *MobiHoc '06: Proceedings of the 7th ACM international symposium on Mobile ad hoc networking and computing*, pages 190–201, New York, NY, USA, 2006. ACM.

[13] Zhibin Wu and Dipankar Raychaudhuri. D-lsma: Distributed link scheduling multiple access protocol for qos in ad-hoc networks. In *Ad-hoc Networks,âAu Proc. Globecom 2004*, pages 1670–1675, 2004.